IOP Publishing Journal of Physics D: Applied Physics
J. Phys. D: Appl. Phys. **40** (2007) 3335–3342 doi:10.1088/0022-3727/40/11/012

Mechanical properties of a 3C-SiC film between room temperature and 600 °C

Michele Pozzi[1], Musaab Hassan[1,5], Alun J Harris[1], Jim S Burdess[2], Liudi Jiang[3], Kin K Lee[3], Rebecca Cheung[3], Gordon J Phelps[1], Nick G Wright[1], Christian A Zorman[4] and Mehran Mehregany[4]

[1] School of Electrical, Electronic and Computer Engineering, Newcastle University, NE1 7RU, UK,
[2] School of Mechanical and Systems Engineering, Newcastle University, NE1 7RU, UK
[3] School of Engineering and Electronics, Scottish Microelectronics Centre, The University of Edinburgh, EH9 3JF, UK
[4] Microfabrication Laboratory, Department of Electrical Engineering and Applied Physics, Case Western Reserve University, Cleveland, OH 44106, USA

E-mail: michele.pozzi@ncl.ac.uk

Received 2 March 2007
Published 18 May 2007
Online at stacks.iop.org/JPhysD/40/3335

Abstract
Silicon carbide (SiC) is widely recognized as the leading candidate to replace silicon in micro-electro-mechanical systems devices operating in harsh environments. In this work, cantilevers and bridges in SiC are designed, fabricated and evaluated between room temperature (RT) and 600 °C. The active material is a cubic poly-SiC film deposited on a poly-Si layer which is separated from the Si substrate by a thermal oxide. From surface profiling and optical observations, it is deduced that an average residual strain of $+5 \times 10^{-4}$ is present in the 2.7 μm thick film, with a gradient of 2.5×10^{-4} μm^{-1}. The structures are excited either mechanically or electrostatically. Their resonance frequency is measured by laser Doppler velocimetry and used to derive the Young's modulus and residual stress in the heteroepitaxial layer (330 ± 45 GPa and 200 ± 20 MPa, respectively). The temperature coefficient of Young's modulus is found to be -53 ± 2 ppm K^{-1} in the range RT to ~300 °C, while an analytical expression is given for the temperature dependence of the Young's modulus between RT and 500 °C. The residual tensile stress is found to depend on temperature in a complex manner.

1. Introduction

In recent years, silicon carbide (SiC) has emerged as a valid alternative to silicon (Si) for micro-electro-mechanical systems (MEMS) operating in harsh environments due to its superior mechanical, physical and chemical properties [1,2]. Although a very large number of SiC polytypes have been identified, only a few of them have found significant technological application. In SiC electronics, polytypes with hexagonal symmetry (such as 4H and 6H) are commonly used, as single-crystal wafers are commercially available. The only possible cubic polytype (3C-SiC or β-SiC according to an older nomenclature) is superior to the other polytypes in some respects (e.g. higher electron mobility), but it is proving more difficult to grow in high quality single crystals [3]. A two-step technique, carbonization followed by chemical vapour deposition, has been refined in the past decade to deposit 3C-SiC films on Si. Although a considerable mismatch between the lattice parameters of Si and SiC renders the interface highly defective, the properties of the deposited film are still superior to those of silicon. Furthermore, the deposition technique permits the build-up of layered materials which can prove much more convenient for the fabrication of MEMS.

[5] Present address: Faculty of Biomedical Engineering, Academy of Medical Sciences and Technology, PO Box 12810, Khartoum, Sudan.

Although SiC is advantageously more stable at extreme temperatures than Si, mechanical, electronic and dimensional changes can be important when the fabricated devices are required to operate over a wide temperature range. It is therefore necessary to characterize the material not only at a fixed temperature but also as a function of temperature.

From the mechanical point of view, the dependence of the Young's modulus on temperature should be a primary concern. In a simple 'static' device, such as an accelerometer with proof mass, a decrease in the Young's modulus with temperature means that a systematic overestimation of the acceleration will take place at high temperature. A similar effect would be seen with a membrane pressure sensor. Dynamic sensors, where the quantity to measure produces a shift in the natural frequency of a resonator, are also affected. In fact, the resonance frequency of a cantilever can change by over 1% over a 500 K range, which is highly significant for precise measurements. Whereas part of this change is due to dimensional variations caused by thermal expansion, the great majority of it is due to a reduction in Young's modulus. One of the first determinations of the temperature coefficient of Young's modulus (TCYM) of 3C-SiC films is given by Su *et al* [4]. Their work focused on single-crystal 3C-SiC epitaxially grown on Si, for which they found a value of $-46\,\mathrm{ppm\,K^{-1}}$ for the undoped material in the range between room temperature (RT) and ∼450 °C. However, due to lower costs, polycrystalline 3C-SiC is more commonly found in material structures suitable for surface micromachining. The focus of this paper, therefore, is the layered structure where the 3C-SiC is deposited epitaxially on poly-Si, which functions as the sacrificial layer in the MEMS fabrication process.

Because of the widespread acceptance of Si and the relative novelty of SiC, the difference in quantity and quality of available data about the two materials is very significant. The aim of this paper is to contribute to bridging this gap, by reporting on the characterization of a multilayered poly-3C-SiC structure suitable for surface micromachining. In particular, we have determined the residual stress, stress gradient and the Young's modulus, and its dependence on temperature, of a polycrystalline 3C-SiC film grown according to the two-step technique mentioned above.

The present paper summarizes results found with two different experimental arrangements and on differently prepared devices. They will be denoted in the following as 'setup 1' and 'setup 2'.

2. Experimental details: setup 1

The material is a 2.7 μm thick SiC undoped film heteroepitaxially deposited on a layered structure composed of a single-crystal Si substrate (∼500 μm), a SiO_2 insulating layer (∼1.5 μm) and a poly-silicon sacrificial layer (∼3.7 μm), as shown schematically in figure 1. SNMS analyses revealed a typical composition of $Si_{44\%}C_{56\%}$ for the SiC film, which was grown at high temperature following a carbonization step of the underlying poly-Si.

Cantilever structures, figure 2(*a*), were used to determine the value of Young's modulus and its dependence upon temperature. Bridges, figure 2(*b*), together with a strain measuring device, figure 2(c), were used to measure the residual stress and strain, and this provided an alternative method to derive the value of Young's modulus. The operation of the strain measuring device, which is inspired by the structures presented in [5], is very simple. Upon etching, the perforated beams are free to contract or expand. This causes a relative displacement of the central indicator beams which was measured using a simple image processing of an optical micrograph. This displacement was directly correlated to strain by FEA and an analysis of the linkage mechanism.

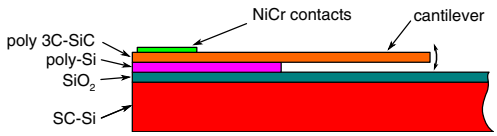

Figure 1. Schematic cross-section view of the material used to fabricate the devices. The poly-Si acts as the sacrificial layer, whilst the oxide offers electrical insulation between devices and substrate.

Fabrication of the devices was performed by etching the SiC film using a one-step inductively coupled plasma (ICP) etching technique that also removes the underlying poly-Si, releasing the devices [6]. Silicon dioxide was used as the etching mask. NiCr contacts were deposited near the edges of the die to permit the electrostatic actuation of the SiC devices by virtue of the electric field between the SiC beam and the Si substrate, see figure 1.

The experimental apparatus used to conduct dynamic tests on the SiC beam structures is shown in figure 3. An evacuated chamber contains a heating element on which the sample is placed. The walls of the small cavity housing the sample are covered in silver foil to reflect thermal radiation. Virtually all the remaining volume of the chamber is filled with thermally insulating ceramic (Duratec®). The structures can be viewed from above through a 'hot mirror', whose special coating reflects most of the infra-red radiation but is transparent to the visible light. The collimated beam of a laser Doppler velocimeter (LDV) is focused onto the devices through a modified microscopic objective that enables simultaneous optical observation.

The pressure within the test chamber was continually monitored during the measurements and was noted to increase from 0.02 to 0.5 mbar as the temperature was increased to 600 °C. This pressure variation was caused by further degassing of the insulating material, even after baking, and could not be eliminated. To ascertain its effects on the resonance frequency, a cantilever's vibration was monitored at room temperature while the pressure was changed over a wider range. This test showed that the pressure variations known to take place inside the chamber during thermal cycling produce a change in frequency below 80 ppm. The corresponding shift in frequency caused by temperature changes from ∼20 to 600 °C was 200 times greater.

Precise temperature control of the die was achieved by placing the die on a specially designed resistive heater. The heater was constructed from two 1 mm thick plates of Macor® ceramic and a serpentine of NiCr wire bonded together as a sandwich by a filling of a suitable high temperature binder. The die was placed directly onto the top ceramic plate and was clamped firmly down by two small steel clips. In order to minimize stresses of external origin, the clips were not applied

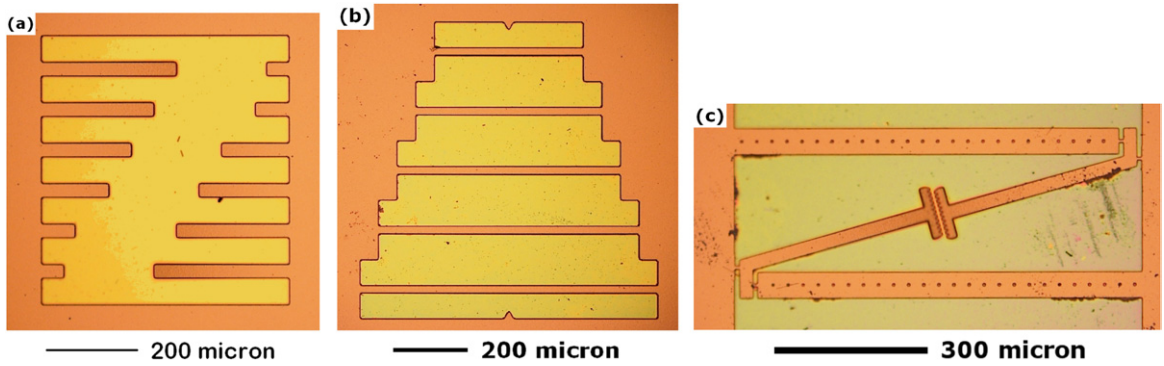

Figure 2. Optical photographs of some of the devices fabricated: (*a*) cantilevers with lengths between 50 and 500 μm, (*b*) bridges with lengths between 400 and 800 μm and (*c*) the strain measuring device.

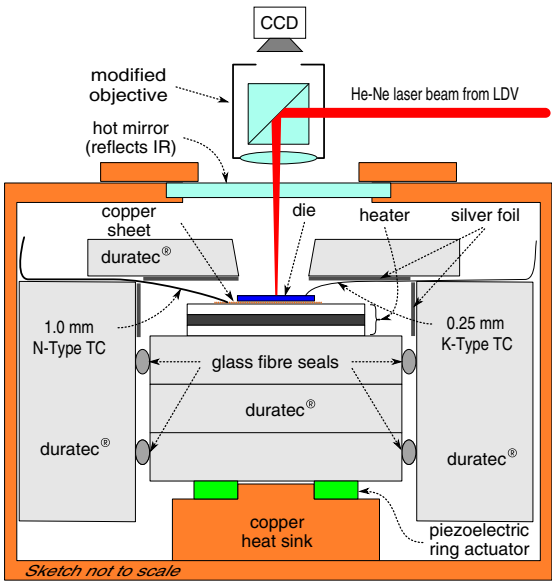

Figure 3. Sketch of the cross section of experimental setup 1, used for the characterization of the devices at different temperatures. The leads needed for electrostatic actuation and those that supply the heating element are omitted. Mechanical excitation is by means of the piezoelectric ring actuator located in the lower part of the assembly.

while measuring the resonance frequency of a bridge as a function of temperature. As the lack of a firm clamping system limited the accelerations that could be applied, only some of the bridges could be tested in this manner. For electrostatic excitation a thin copper sheet was positioned between the die and the heater to enable electrical contact to the substrate.

To monitor the surface temperature of the die, a mineral insulated type K thermocouple with external diameter 250 μm was placed in contact with the top surface of the sample and was held in position by elastically preloading it against the surface. A second mineral insulated thermocouple (type N, diameter 1 mm) was placed a couple of millimetres away from the die, in close contact with either the ceramic plate or copper sheet. The type K thermocouple was used to provide feedback to a PID-based temperature controller, whilst the type N thermocouple was independently monitored. It was assumed that the real temperature of the devices (T_R) lies near the two values read (T_N and T_K), with T_K providing a more accurate reading. A simple heat transfer analysis of the setup shows that thermal energy flows through the chip constantly, entering from the bottom, diffusing through its small thickness (mostly Si) and then being radiated from the top SiC surface as well as conducted along the steel clips, the electrical lead and the 250 μm thermocouple itself. At higher temperature, an important channel of heat loss is represented by radiation. For this reason, the heater/sample system was surrounded by insulating/reflecting material, as detailed above. It was expected that the surface of the heater would be hotter than the surface of the chip; this was almost always observed experimentally, with T_N–T_K becoming greater than 50 K at the highest temperatures when the copper sheet was present. On the other hand, when the sample was directly contacting the heater, this gradient was much lower, with $T_N \approx T_K$ up to 500 °C.

It is also worth noting that the suspended cantilevers radiate energy along their length, whilst receiving heat mostly through their root. As a consequence, a temperature gradient of a few degrees may exist between root and tip. An expression for the temperature profile of the cantilever was derived by equating, for each point along the cantilever, the heat conducted through the cross section at that point and the heat radiated by the top surface from that point to the tip. It was found that, due to the high thermal conductivity of SiC, the temperature difference at 900 K is less than 1 K. This effect would be more important for materials with lower thermal conductivities or for thinner devices.

Following these considerations, it was decided to assume the temperature of the devices to be equal to T_K, with an estimated uncertainty ranging from ± 5 K at low temperature to ± 25 K at the highest temperature—these also include the intrinsic uncertainties of the thermocouple wire and of the measuring equipment.

The beams were forced into flexural vibration using either electrostatic or mechanical excitation. An electrostatic drive is normally easier to achieve provided the devices are sufficiently conducting and there is provision for electrical contacts. It also enables high vibration amplitudes to be produced. The disadvantages of the method are the insulating oxide may fail at high temperatures and there is the possibility of a build-up of DC fields, for example, caused by imperfect ohmic contacts which will alter the excitation characteristics of the actuation.

Mechanical excitation requires a more complex experimental apparatus, particularly when tests are performed at high

temperatures. Mechanical excitation was effected by a piezoelectric multilayer actuator, separated from the die by several centimetres of thermally insulating ceramic, to ensure it was kept within its environmental limits of operation (see sketch in figure 3).

For both the actuation methods, excitation was achieved with a swept sine signal and the vibration amplitude was kept to the minimum necessary to clearly identify the resonance peaks.

The velocity of vibration was measured with a LDV, whose probe beam was directed into a modified objective mounted on an interferometric microscope. This setup permitted accurate positioning of the laser spot on the device of interest. Typical speed amplitudes of 5–10 mm s^{-1} were measured at a point about 50 μm from the root of the cantilevers; twice as large values were typical in the middle of the bridges. The LDV output was digitized with an oscilloscope PCI card. Specially developed software performed a Fast Fourier Transform (FFT) of the temporal data and enabled the automatic detection of the peaks in the computed spectrum. The peaks position was plotted in real-time to enable the observation of their evolution with time during the heating steps.

3. Experimental details: setup 2

A chip of a similar material was used to fabricate cantilevers used to determine the TCYM. In this case, the $Ni_{0.8}Cr_{0.2}$ layer was all over the SiC, hence the devices were bi-layer structures and the analysis of their data requires special methods. The chip was placed on a heater, whose inner temperature was monitored and assumed to be the temperature of the cantilevers. The assembly was placed in a high vacuum chamber. Electrostatic excitation was achieved applying a biased sinusoidal voltage ranging between 0 and 400 mV. The velocity of vibration was measured with the LDV mentioned above.

4. Results and discussion: setup 1

Initial observation with a surface profilometer showed that the cantilevers are bent upwards, with a radius of curvature of $r = 4.0 \pm 0.1$ mm. This indicates the existence of a strain gradient through the thickness. A simple calculation, based upon simple bending theory, reveals that the bending can be explained by the relaxation of an average stress gradient equal to

$$\frac{\Delta\sigma}{\Delta t} = \frac{E}{r} = (92 \pm 10)\ \text{MPa}\ \mu\text{m}^{-1},$$

assuming $E = 370 \pm 40$ GPa.

One device was removed from the die and placed flat on a reference surface; by profiling the area of contact it was possible to measure the thickness, which was found to be in excellent agreement with the average value deduced from SEM images. A value of thickness equal to 2.7 ± 0.1 μm was calculated by combining these two values.

Clamped-clamped beams of varying lengths between 400 μm and 4 mm were manufactured on the same chip for the purpose of measuring the residual tensile stress in the SiC film. This stress is caused by the lattice mismatch between Si and SiC and the thermal strain due to the fact that the SiC film was deposited at a high temperature. A total of 47 bridges were tested, and these were selected from two groups which were set orthogonally to each other on the die.

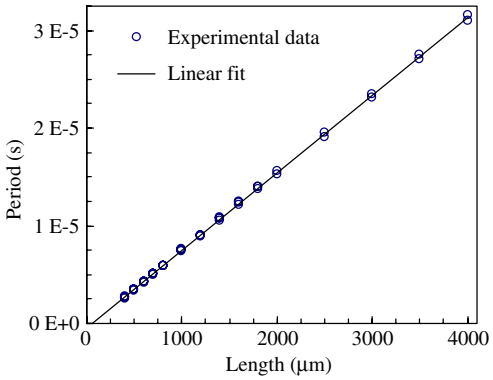

Figure 4. Fundamental period of vibration versus design length of 47 bridges.

A very good linear correlation between the period of vibration and the length, figure 4, was observed when the bridges were mechanically excited in their first mode. The equation fitting the data, with l expressed in μm, is

$$T_r = a \cdot (l + l_0) = (7.95 \pm 0.02) \times 10^{-9} \times [l - (59 \pm 4)],$$

$$R^2 = 0.9997.$$

This linear dependence, which is evidence of string-like behaviour, is expected as the bridges are very long compared with their thickness and are also under considerable tension (interestingly, a small deviation from this model due to beam stiffness can be noted on analysing the residuals of the fit, which discriminate long and short bridges).

The fundamental resonance frequency of a taut string is simply

$$f_r = \frac{1}{2l}\sqrt{\frac{\sigma}{\rho}},$$

so that the slope of the linear fit is given by

$$a = 2\sqrt{\frac{\rho}{\sigma}}.$$

Assuming[6] a tabulated value of $\rho = (3150 \pm 10\%)$ kg m^{-3}, one can calculate that the bridges are under an average tensile stress $\sigma = 200 \pm 20$ MPa. This is a considerably large stress, and varies with temperature in a complex manner, as shown in figure 5. The stress increases with temperature until about 100 °C, thereafter a reduction in stress was observed with increasing temperature. The calculation of stress from the FEA of a bridge using published values of coefficients of thermal expansion for SiC [7] and poly-Si [8, 9] agrees qualitatively with this behaviour, as can be seen in the same plot. However, it must be stated that the model took no account of the thermal expansion of the SiO_2 film. Experimentally, it was noted that the stress continued to change for 10–20 min after a satisfactory constant temperature was reached, suggesting that complex

[6] Deviations from the tabulated value may arise from crystallinity, composition and microstructure.

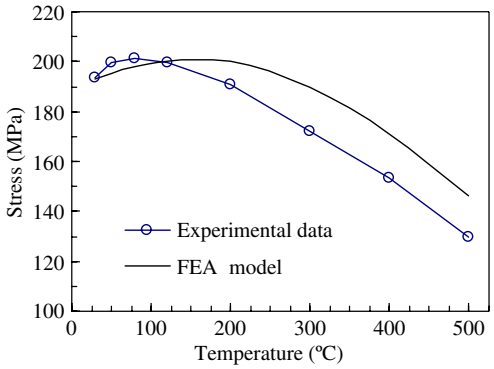

Figure 5. Tensile stress in an 800 μm long bridge as a function of temperature.

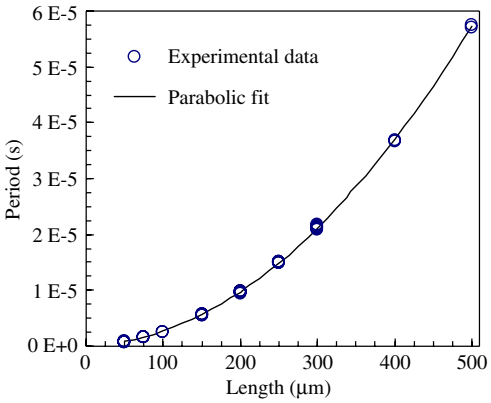

Figure 6. Period of first normal mode of vibration of 35 cantilevers as a function of their length.

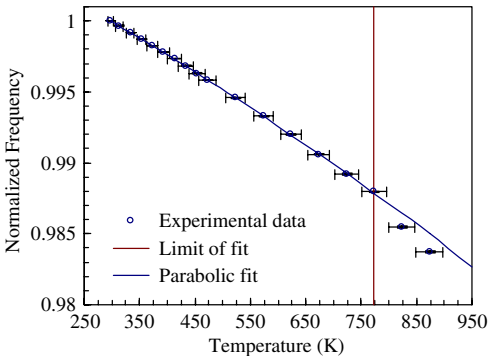

Figure 7. Normalized frequency versus temperature: experimental data and quadratic fit. Each point is the average of the values collected at that temperature on 8 different cantilevers. The vertical error bars (barely noticeable) are equal to the standard deviation of these values. The horizontal error bar reflects the estimated uncertainties on the temperature measurement. The vertical line marks the limit of the data used for the analytical fit.

time-dependent phenomena take place. This unexplained behaviour suggests that extracting the TCYM from bridges would be very challenging. However, because the tensile stress relaxes in a cantilever, this behaviour is not expected to have any significant effect on the TCYM derived from cantilever data.

The strain measuring device fabricated on the same chip, figure 2(*c*), showed that the strain relaxation upon etch-release is approximately equal to 5×10^{-4}. Using this strain value with the tensile stress measured from the bridges, a value of Young's modulus equal to $E = \sigma/\varepsilon = 400 \pm 50$ GPa can be calculated.

A set of 35 cantilevers was present on the chip. Their lengths ranged between 50 and 500 μm, whilst their widths were either 20 or 30 μm. The period of their fundamental mode is plotted against length in figure 6 and follows the quadratic behaviour expected from the simple vibration theory. The equations fitting the data are

$$T_r = a(l + l_0)^2 = (2.195 \pm 0.01) \times 10^{-10} \times [l + (10.5 \pm 0.8)]^2,$$

$$R^2 = 0.999\,86,$$

where the parameter l_0 is introduced in the squared term to signify that the length of the cantilevers may be viewed as the total of the design length and a fixed length which is related to the undercut. The parameter a is related to the thickness h, the Young's modulus $E$and the density ρ by the following expression, derived from the well-known frequency equation of the cantilever vibrating in its fundamental mode:

$$a \approx \frac{4\pi}{(1.875)^2\, h}\sqrt{\frac{3\,\rho}{E_e}},$$

where $E_e = (1-\nu^2)E$ and $\nu = 0.16$ is the Poisson's ratio. This equation can be used to deduce that $E = 330 \pm 45$ GPa. This value of Young's modulus is in reasonable agreement with the value of $E = 400 \pm 50$ GPa, obtained from the data provided by the bridges and the strain measuring device.

For the determination of the TCYM, the resonance frequency of a subset of cantilevers was measured at different steady temperatures. Figure 7 shows the average of the normalized resonance frequency of 8 cantilevers for one particular run, where the temperature was set between 22 and 600 °C. Only data up to a temperature of 500 °C are used in the analytical fit, as an anomaly clearly appears beyond that value. The fit is almost linear, but the data are accurate enough to clearly bring out a second order dependence. It is therefore worthwhile making a non-linear analysis, also because the coefficient of thermal expansion (CTE) is known to be non-linear [7]. A least-square fit with a 2nd-order polynomial gives

$$f/f_0 = (1.0063 \pm 0.0002) + (-1.95 \pm 0.06) \times 10^{-5} T,$$
$$+ (-5.7 \pm 0.5) \times 10^{-9}\, T^2,$$
$$R^2 = 1 - 9 \times 10^{-5} = 0.99991, \qquad (1)$$

where T is expressed in kelvin.

If the temperature dependence of a generic linear dimension is written as $l(T) = l_0\, \gamma(T)$ and we also write $E = E(T)$, so that $\gamma(T_0) = 1$ and $E(T_0) = E_0$ for an arbitrary reference temperature T_0, the resonance frequency of a cantilever vibrating in mode n can be written as

$$f_n = \frac{(k_n l)^2}{4\pi}\frac{h}{l^2}\sqrt{\frac{E}{3\rho}} = \frac{(k_n l)^2}{4\pi}\sqrt{\frac{w_0 h_0^3}{l_0^3}}\sqrt{\frac{E(T)\,\gamma(T)}{3\,m}},$$

where w, h and l are the width, thickness and length of the cantilever, respectively. It is then possible to divide this expression by f_n calculated at the reference temperature T_0

yielding

$$\frac{f_n}{f_{n,0}} = \sqrt{\frac{E(T)}{E_0}\,\gamma(T)}.$$

We can now drop the subscript n because there is no more dependence on the mode order; then, solving for $E(T)$,

$$E(T) = E_0 \frac{(f/f_0)^2}{\gamma(T)}. \tag{2}$$

The scaling factor $\gamma(T)$ is a function of the instantaneous CTE, $\alpha(T)$:

$$\gamma(T) = \exp\left[\int_{T_0}^{T} \alpha(T)\mathrm{d}T\right].$$

Expression (2) completely describes the dependence of the Young's modulus on temperature in the range from RT to ~800 K, as the ratio f/f_0 is the experimental curve plotted in figure 7.

The expression for $E(T)$ given in (2) can be satisfactorily approximated with a more manageable polynomial. To derive this expression, the quadratic fit to the experimental data f/f_0, given in (1), was used. As for $\alpha(T)$, the semi-empirical formula from [7] was used. Experimental errors in the CTE data are not so important for the present derivation because the total effect of the CTE on the calculated TCYM is less than 10%. The approximate expression for $E(T)$, found by a least-square adaptation of a polynomial to the analytical curve and valid between room temperature and approximately 800 K, is given by

$$E(T) = (-1.3 \times 10^{-8}T^2 - 4.1 \times 10^{-5}T + 1.0134)E_0. \tag{3}$$

In some situations it may be more convenient to have an expression for the instantaneous TCYM. One way to derive it is by differentiating the logarithm of (2):

$$\mathrm{TCYM}(T) \equiv \frac{\mathrm{d}\,E(T)}{E(T)} = 2\frac{\mathrm{d}\,f(T)}{f(T)} - \alpha(T)\mathrm{d}T. \tag{4}$$

Figures 8(*a*) and (*b*) show the graph of the functions $E(T)/E_0$ and $\mathrm{TCYM}(T)$, respectively. A simple second order approximation to (4) can be written as

$$\mathrm{TCYM}(T) = 7.6 \times 10^{-12}T^2 - 3.8 \times 10^{-8}T - 3.7 \times 10^{-5}. \tag{5}$$

This is found by fitting a polynomial to the analytical curve and yields excellent results between room temperature and approximately 800 K.

As previously mentioned, the fit on the data presented in figure 7 is extremely good, which suggests that there are very small random errors present in each run. It is however important to report that greater variability was found between runs where the mounting suffered modest variations (e.g. with or without the copper sheet). This means that there may be systematic errors within each set of data, which cannot be highlighted by the least-squares fit. The most likely source of these errors is the measurement of high temperatures. On the other hand, it is reassuring that the slope was found to be the same, within 0.5%, for mechanical and electrostatic excitation, and it was equally unaffected by the direction of temperature ramp. The slopes of f/f_0 versus T for data collected in several runs for temperatures between RT and 300 °C fall in the range -24.3 to $-26.6\,\mathrm{ppm\,K^{-1}}$, with different degrees of uncertainty. Thus the best estimate for the $\mathrm{d}f/f_0$ for this temperature range is $(-25 \pm 1)\,\mathrm{ppm\,K^{-1}}$. As the temperature range now being considered is relatively narrow, a linear approximation is advisable and therefore (4) can be written without including the temperature dependence. By taking an average value of $3 \pm 1\,\mathrm{ppm\,K^{-1}}$ for the CTE, the temperature coefficient of Young's modulus in the range RT to 300 °C can be written as

$$\mathrm{TCYM} = 2\frac{\mathrm{d}\,f_n}{f_n} - \alpha = -(53 \pm 2)\,\mathrm{ppm\,K^{-1}}.$$

This value compares well with the value of $-46\,\mathrm{ppm\,K^{-1}}$ found by Su *et al* [4] on single-crystal material. It is also interesting to compare it with the values for poly-silicon, which range between -32 [10] and $-75\,\mathrm{ppm\,K^{-1}}$ [11].

The uncertainties given above were determined for a 67% confidence level.

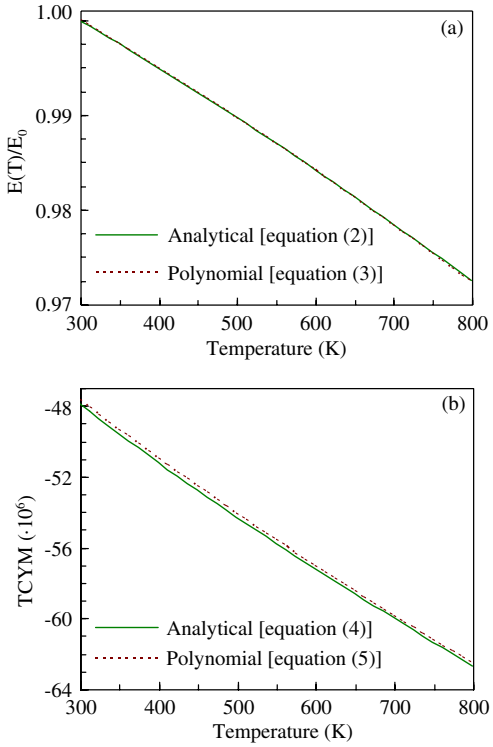

Figure 8. (*a*) Graph of the normalized Young's modulus in the range of validity. (*b*) Graph of the temperature coefficient of Young's modulus in the same range. In both the cases, analytical curve and polynomial approximation almost overlap.

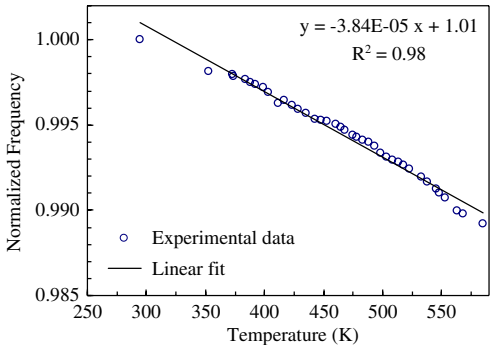

Figure 9. Normalized resonance frequency versus temperature of a cantilever in setup 2.

5. Results and discussion: setup 2

Figure 9 shows the dependence of the resonant frequency with temperature. A linear regression on the curve shows a slope of -84 ppm K^{-1}. In this case, extraction of the TCYM for SiC is more involved, because of the effects of the NiCr layer. There are previous examples of attempts to take this second layer into account. Jianqiang *et al* [12] used a simple averaging method, whereby the Young's modulus of the multilayered cantilever is assumed to equal the weighted average of the Young's moduli of the constituting materials, using their thickness as weight. This approach will only be acceptable when the respective Young's moduli are similar. However, if they are significantly different, it is necessary to consider the fact that the neutral axis is not in the middle of the beam. A more accurate description was reported by Sandberg *et al* [13]. When applied to the cantilevers of setup 2, the equation numbered '14' in their work becomes

$$f_1 \approx \frac{(1.8751)^2}{2\pi l^2}\left\{\left(E_{\mathrm{SiC}}\int_0^{h_{\mathrm{SiC}}}(z-z_0)^2\,\mathrm{d}z + E_{\mathrm{NiCr}}\int_{h_{\mathrm{SiC}}}^{h_{\mathrm{SiC}}+h_{\mathrm{NiCr}}}(z-z_0)^2\,\mathrm{d}z\right)\times\left(h_{\mathrm{SiC}}\rho_{\mathrm{SiC}}+h_{\mathrm{NiCr}}\rho_{\mathrm{NiCr}}\right)^{-1}\right\}^{1/2}. \tag{6}$$

The position z_0 of the neutral axis is the solution to the following equation:

$$E_{\mathrm{SiC}}\int_0^{h_{\mathrm{SiC}}}(z-z_0)\,\mathrm{d}z + E_{\mathrm{NiCr}}\int_{h_{\mathrm{SiC}}}^{h_{\mathrm{SiC}}+h_{\mathrm{NiCr}}}(z-z_0)\,\mathrm{d}z = 0.$$

Every parameter x_k in equation (6) is a function of temperature, so that the variation of the resonance frequency about a specific temperature T_0 can be expressed in the form

$$\mathrm{d}f_1 = \sum \left.\frac{\partial f_1}{\partial x_k}\right|_{x_k=x_{0k}} x_{0k}\alpha_k\,\mathrm{d}T, \tag{7}$$

where α_k is the first order temperature coefficient of parameter x_k and $x_{0k} = x_k(T_0)$. From (7), the TCYM of SiC can be found. Table 1 summarizes the values used for the calculation; the materials' properties are typical values found in the literature and they are assumed to describe the materials used to within $\pm 10\%$, except when stated otherwise. The calculated value of TCYM is $-(49 \pm 18)$ ppm K^{-1}.

Table 1. Parameters used to calculate the TCYM of SiC for the devices in setup 2.

Parameters	Values
E_{SiC}	370 GPa
α_{SiC}	3 ± 1 ppm K^{-1}[a]
h_{SiC}	$2.1 \pm 0.6\ \mu$m[b]
ρ_{SiC}	3150 kg m^{-3}
E_{NiCr}	186 GPa
α_{NiCr}	15 ppm K^{-1}
h_{NiCr}	$0.25\ \mu$m^{-1}[c]
ρ_{NiCr}	8300 kg m^{-3}
TCYM$_{\mathrm{NiCr}}$	-300 ppm K^{-1}

[a] Calculated from [7].
[b] Measured on wafer.
[c] Estimated from deposition time.

6. Conclusions

Conscious design of SiC MEMS devices operating at high temperatures requires knowledge of the mechanical properties of the material as a function of temperature. In this work, test devices in SiC were designed, fabricated and evaluated over a wide temperature range.

The Young's modulus of SiC was seen to decrease with increasing temperature at a rate of -53 ± 2 ppm K^{-1} between RT and $\sim$300 °C, in good agreement with results previously reported by other authors. For the first time, a more accurate non-linear expression is given to describe the temperature dependence of Young's modulus for the range between RT and $\sim$800 K. This information is valuable when designing devices capable of predictable operation over a wide range of temperatures.

The resonance frequency of free-standing devices is shown to be affected by this decrease in Young's modulus, with minor additional effects arising from dimensional changes due to thermal expansion. In over-constrained devices, such as bridges, the resonance frequency depends on temperature in a complex manner, dominated by variations in tensile stress due to differential thermal expansion between SiC and substrate. It is therefore advised that mechanical designs avoid stressed members or rather employ a topology which permits the relaxation of the residual tensile stress in active elements.

The results reinforce the view that although SiC is a mechanically superior material to Si for application at high temperatures, the designer must be aware of the change of its mechanical properties with temperature, as this will cause variations in performance at different temperatures.

Acknowledgment

The authors acknowledge the support of the Engineering and Physical Sciences Research Council (EPSRC) through grant No GR/T06339/01.

References

[1] Mehregany M, Zorman C A, Roy S, Fleischman A J, Wu C H and Rajan N 2000 Silicon carbide for microelectromechanical systems *Int. Mater. Rev.* **45** 85–108

[2] Casady J B and Johnson R W 1996 Status of silicon carbide (SiC) as a wide-bandgap semiconductor for high-temperature applications: a review *Solid-State Electron.* **39** 1409–22
[3] Jayatirtha H N, Spencer M G, Taylor C and Greg W 1997 Improvement in the growth rate of cubic silicon carbide bulk single crystals grown by the sublimation method *J. Cryst. Growth* **174** 662–8
[4] Su C M, Wuttig M, Fekade A and Spencer M 1995 Elastic and inelastic properties of chemical vapor deposited epitaxial 3C-SiC *J. Appl. Phys.* **77** 5611–15
[5] Schweitz J-A and Ericson F 1999 Evaluation of mechanical materials properties by means of surface micromachined structures *Sensors Actuators A: Phys.* **74** 126–33
[6] Jiang L, Cheung R, Hassan M, Harris A J, Burdess J S, Zorman C A and Mehregany M 2003 Fabrication of SiC microelectromechanical systems using one-step dry etching *J. Vac. Sci. Technol.* B **21** 2998–3001
[7] Reeber R R and Wang K 1996 Thermal expansion of β-SiC, GaP and InP *Symp. on Covalent Ceramics III - Science and Technology of Non-Oxides (Boston, MA, USA)* ed A F Hepp *et al* (Pittsburg, PA: Materials Research Society) pp 211–16
[8] Reeber R R and Wang K 1996 Thermal expansion and lattice parameters of group IV semiconductors *Mater. Chem. Phys.* **46** 259–64
[9] Roberts R B 1981 Thermal expansion reference data: silicon 300–850 K *J. Phys. D: Appl. Phys.* **14** L163–6
[10] Biebl M, Brandl G and Howe R T 1995 Young's modulus of *in situ* phosphorus-doped polysilicon *Proc. Int. Conf. on Solid-State Sensors and Actuators, and Eurosensors IX (Stockholm, Sweden)* (Piscataway, NJ: IEEE) pp 80–3
[11] Guckel H, Burns D W, Tilmans H A C, DeRoo D W and Rutigliano C R 1988 Mechanical properties of fine grained polysilicon - the repeatability issue *IEEE Solid-State Sensor and Actuator Workshop (Hilton Head Island, SC, USA)* (Piscataway, NJ: IEEE) pp 96–9
[12] Jianqiang H, Changchun Z, Junhua L and Yongning H 2002 Dependence of the resonance frequency of thermally excited microcantilever resonators on temperature *Sensors Actuators A: Phys.* **101** 37–41
[13] Sandberg R, Svendsen W, Molhave K and Boisen A 2005 Temperature and pressure dependence of resonance in multi-layer microcantilevers *J. Micromech. Microeng.* **15** 1454–8